Density functional theory study on the hydrodesulfurization reactions of COS and CS$_2$ with Mo$_3$S$_9$ model catalyst

Xiao-Qian Yao [a,*], Yong-Wang Li [b]

[a] Research Laboratory of Green Chemistry and Technology, Institute of Process Engineering, Chinese Academy of Sciences, 100190 Beijing, China
[b] The State Key Laboratory of Coal Conversion, Institute of Coal Chemistry, Chinese Academy of Sciences, 030001 Taiyuan, China

ABSTRACT

The catalytic hydrodesulfurization (HDS) reactions of COS and CS$_2$ with Mo$_3$S$_9$ cluster have been systematically investigated as a part of HDS of industrial feedstocks by DFT-based method. A detailed description of mechanisms is given, and different pathways are discussed and compared. It is found that the S in COS and CS$_2$ will be hydrogenated, and the reactions will lead to formations of H$_2$S, CO and CS. Comparing with COS, CS$_2$ reacts with lower activation free energy and shows more reaction activity.

© 2008 Elsevier B.V. All rights reserved.

1. Introduction

Hydrodesulfurization (HDS) of petroleum feedstocks is catalytic removal of sulfur by the use of H$_2$ from sulfur-containing compounds [1]. The sulfur content of industrial feedstocks not only affects the environment, but also provides economic problems within the petrochemical industry. Thiols, thiophenes and carbonyl sulfide, etc. are the compounds commonly encountered irrespective of the origin of the petroleum [2]. While the sulfur in petroleum can be found in a variety of species, compounds containing the thiophene ring are of special interest since they are the most difficult to desulfurize due to their stabilization [3]. In recently years, there also has been renewed interest in carbonyl sulfide hydrogenation and the processes used to remove sulfur from chemical feedstocks for environmental and industrial reasons [2].

As we know, promoted catalysts based on molybdenum sulfides are commonly used for the HDS process. The molybdenum sulfide (MoS$_2$ or more precisely MoS$_x$ under the reductive atmosphere) catalyst is usually used to study the HDS of organosulfur compounds [4–7]. However, there are very less paper on reaction between the molybdenum catalyst with other sulfur-containing compounds, such as carbonyl sulfide and carbon disulfide. In Rhodes's paper, among different COS and CS$_2$ removal methods, an alternative proposal to reduce the levels of COS and CS$_2$ is hydrogenation using Co–Mo–Al$_2$O$_3$ type catalyst [2], and the sulfur-containing compounds are reduced to H$_2$S, H$_2$O and CH$_4$, then processed in subsequent steps. Based on the result, it is thought that the S content of COS and CS$_2$ in petroleum-based feedstocks would also be reduced with molybdenum sulfide catalyst in the HDS process. It will be helpful for understanding comprehensively petroleum HDS process to investigate catalyzed reactions of COS and CS$_2$ as a part of the HDS.

In order to understand the relationships between the detailed structures of molybdenum sulfide catalyst surfaces and catalytic activity, numerous theoretical descriptions of MoS$_2$ surfaces under various conditions have been proposed [8–21]. However, the mechanism of catalytic HDS is far away from well understood. Although theoretical calculations can provide detailed information on structures and energies of reactions, computation with a reasonable MoS$_x$ cluster model is too expensive, and a detailed screening of the potential energy surface is very unlikely.

The intermediary *rag* structures of MoS$_x$ catalysts at the initial stages of their formation are considered to contain Mo$_3$S$_9$ cluster units, and these clusters are catalytic active materials. Based on the experimental results [22–24], Weber et al. [25] have proposed four possible Mo$_3$S$_9$ cluster units in triangular form, in which all molybdenum centers have the formal characteristic oxidation state of Mo(IV), and two characteristic Mo–Mo distances as well as two possible kinds of sulfur ligands in different coordination spheres can be identified. The triangular structures of Mo$_3$S$_9$ have been confirmed by the latest quantitative extended X-ray adsorption fine structure studies [26]. These proposed structures have been computed at the density functional level of theory, and two of

* Corresponding author. Tel.: +86 10 62550850; fax: +86 10 82627080.
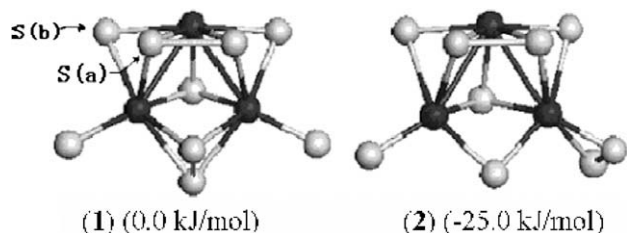E-mail address: xqyao@home.ipe.ac.cn (X.-Q. Yao).

Fig. 1. Two optimized stable structures and relative energies of Mo₃S₉ cluster.

them in close energy are found to be compatible with the experiments as shown in Fig. 1 [27]. The catalytic activity of these small clusters has been observed experimentally by de Bont et al. [28] using NaY zeolite as support to deposit molybdenum-sulfide particles (MoS$_x$) in the NaY supercages for studying the HDS activity of thiophene. At temperatures lower than 673 K, a cluster with two Mo atoms with $R_{Mo–Mo}$ = 2.78 Å (like MoS₃) surrounded by S and denoted as "Mo(2.78 Å)S$_x$" is formed, and this cluster can be transformed into another cluster at 774 K with $R_{Mo–Mo}$ = 3.16 Å (like MoS₂) surrounded by S and denoted as "Mo(3.16 Å)S$_x$". Furthermore, the results indicate that MoS₃-like structure is more active than MoS₂-like structure for HDS. This experiment can validate the use of the Mo₃S₉ cluster in theory calculation for understanding the HDS activity in a reasonable way. As shown in Fig. 1, two Mo₃S₉ clusters are structurally similar and exhibit only a small en-

ergy difference (25.0 kJ/mol). It was supposed that these two Mo₃S₉ isomers might be formed and perhaps could transform to each other when involved in the catalytic process. The more symmetrical unit structure **1** was taken as model catalyst in our study due to this small energy difference.

In our theoretical study of the HDS on Mo₃S₉ cluster [29,30], the catalytic HDS mechanism thiophene and benzothiophene were investigated by density functional theory method. In the thiophene HDS, the calculation results showed that 2,5-dihydrothiophene is the key intermediate and the subsequently formed butadiene is the principal product. For the benzothiophene (BT), it was found that the mechanism of hydrogenation and hydrogenolysis of BT with dihydrobenzothiophene (DHBT) as intermediate is more favored that the direct hydrogenolysis with styrene as intermediate. Despite the limited model size, our results agree well with the available findings. Encouraged by these results, we are also interested in the reactions of molybdenum sulfides with other sulfur-containing compounds in petroleum-based feedstocks, such as carbonyl sulfide and carbon disulfide. However, the reactions of molybdenum sulfides and carbonyl sulfide are very complicated and might be related with many other important catalyst processes while the final products include CH₄. So, the aim of this work concentrates on the hydrodesulfurization reaction activity of COS and CS₂ on Molybdenum sulfide. We have computed hydrodesulfurization part of reaction mechanisms for COS and CS₂ on Mo₃S₉ cluster, and compared the activity of COS, CS₂, thiols, thiophenic compounds on the basis of the calculated free energies of activation and reaction.
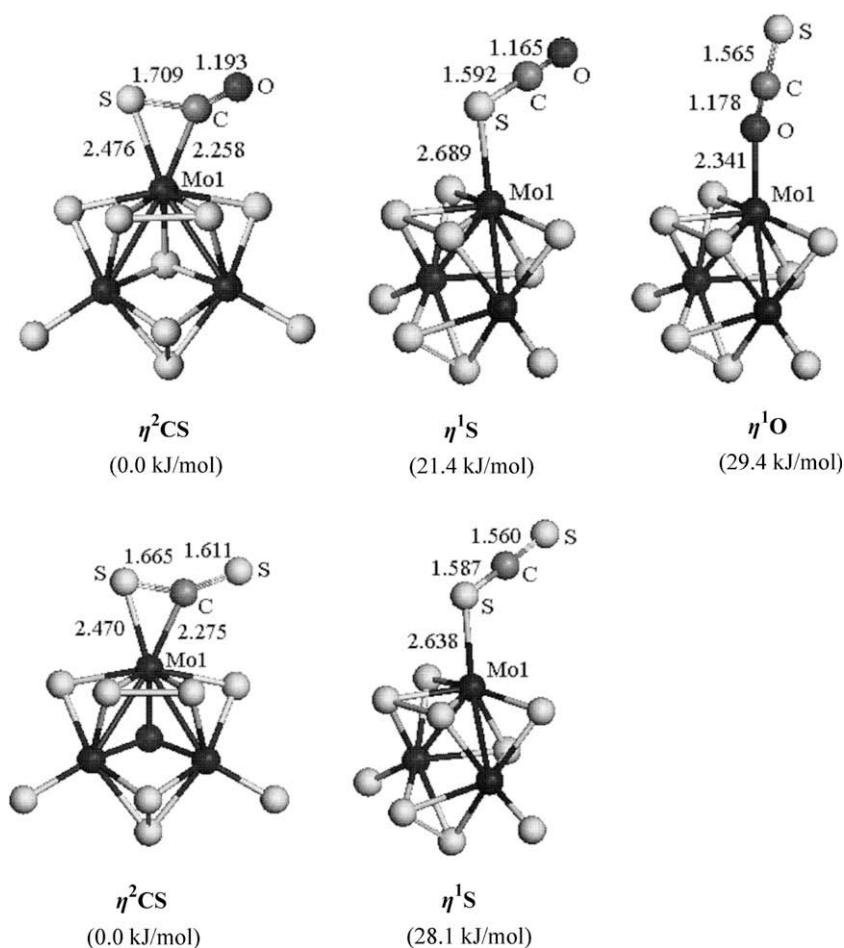

Fig. 2. Optimized structures of adsorbed COS and CS₂ on Mo₃S₉ cluster.

2. Computational details

All calculations were carried out with the DMol program package in the Materials Studio 2.2 of Accelrys Inc. The doubled numerical basis set with d-polarization functions (DND) and the generalized gradient corrected (GGA) functional by Perdew and Wang (PW91) was employed. The mesh size in medium quality for the numerical integration was used, and the tolerances of energy, gradient and displacement convergence were 2×10^{-5} a.u., 4×10^{-3} a.u./Å and 5×10^{-3} Å. The real space cutoff of atomic orbital was set at 5.5 Å. Structures were optimized fully without any constraints. Complete linear synchronous transit and quadratic synchronous transit (LST/QST) calculations were performed to determine structures of transition state (TS), confirmed by additional calculations of the intrinsic reaction path. The corresponding frequencies were computed at the same level in order to check the obtained stationary points to be ground states (minimum structures) with only real frequencies, or to be transition states (maximum structures or saddle points) with only one imaginary frequency displaying the desired displacements orientation and connection. Zero-point energies (ZPE) from the frequency calculations were added to the total energies of each species in the catalytic cycle. To compare with the thiophene HDS study, the Gibbs free energies and the enthalpies of reactions were calculated at same actual experiment condition of 550 K and 1 atm. Considering the entropy effect, our discussions are based on the free energies of activation ($\Delta G^{\ddagger}$) and reaction (ΔG).

3. Results and discussion

Frontier molecular orbital analysis of Mo_3S_9 cluster (**1**) showed that the unsaturated molybdenum center (Mo_1) contributes significantly to the occupied and virtual orbitals and is therefore responsible for the catalytic activity [27]. The Mo_1 is considered to be the active site for HDS. The conformations of coordination complexes in reaction of CS_2 with different metal atoms were discussed in the past theoretical investigation [31,32], three possible adsorption structures that are $\eta^1 S$, $\eta^2 CS$ and $\eta^2 SS$ were proposed. In this work, different adsorption conformations for COS and CS_2 on Mo_3S_9 cluster were investigated and found that there are two kinds of adsorption mode η^1 and η^2. As shown in Fig. 2, three energy minimum adsorption structures for COS are gotten: $\eta^1 S$, $\eta^1 O$, $\eta^2 CS$ (according adsorption coordinated by S, O or C atoms of COS). The energetic differences among them are 21.4 and 29.4 kJ/mol, respectively. It is interesting to found that the $\eta^2 CO$ (coordinated by C and O atoms of COS) is not a stable adsorption structure. Two energy minimum structures of CS_2 that are $\eta^1 S$, $\eta^2 CS$ adsorption mode are also shown in Fig. 2, and the energetic difference for them is 28.1 kJ/mol.

In this work, the hydrogenation steps of COS and CS_2 are studied in a similar way with those of thiophenes with the assumption that atomic hydrogen is available, e.g. mono-hydrogenation on the base of successive atomic H addition. The absorption of H atoms on the surface of MoS_2 was thought to form one Mo–S–H group and probably one Mo–H group [33]. In the calculations, only the surface neighboring Mo–S–H groups were considered, and the monohydrogenated Mo_3S_9H cluster with H close to Mo_1 center was used to coordinate COS and CS_2 for H transfer. Experimentally, the major source of atomic hydrogen is the catalytic dissociation of H_2 by deposited transition metals on MoS_x [34].

3.1. Reaction of COS with Mo_3S_9 cluster

The possible hydrodesulfurization reactions of COS ad CS_2 were considered in this study, and that means only hydrogenations of S

or O were calculated. In our test calculation, it was found that the hydrogenation of S or O cost lower energy than hydrogenation of C and will take place more favored. On the other side, the hydrogenation to C will lead to formation of CH, CH_2 and CH_3 groups, and these reactions will probably form the structures such as CH–SH or CH_3–OH while the hydrogenation of S and O take place at the same time. These reactions will be very complicated and beyond the scope of this paper.

The $\eta^2 CS$ structures of COS and CS_2 were used to calculate the hydrogenation reaction for the lower energy and shorter transferring distance of hydrogen from Mo_3S_9. The adsorbed hydrogen is assumed to transfer to COS and CS_2 from S(a) or S(b) position of Mo_3S_9.

With an H atom attached to the different S atoms closing to the adsorbed COS, four Mo_3S_9H structures with adsorbed COS were calculated, and the optimized geometries are shown in Fig. 3: **1HR(a1)**, **1HR(a2)**, **1HR(b1)** and **1HR(b2)**. They are close in energy with the largest difference of 11.7 kJ/mol, indicating the conformational flexibility. Since the too long transfer distance making the reactions of hydrogen direct transformations to COS in **1HR(a1)** and **1HR(a2)** almost impossible, we will only consider the reactions between H with adsorbed COS in **1HR(b1)** and **1HR(b2)**.

The catalytic hydrodesulfurization of COS has two possible reaction paths: (i) hydrogenation of uncoordinated oxygen, (ii) hydrogenation of coordinated sulfur. The potential energy surface along hydrogenation of uncoordinated oxygen atom of COS is computed firstly. Since adsorption process of atomic H is not taken into account, the free energies for each elementary step are given independently and the corresponding value of reactant for each step is set to 0.0 kJ/mol.
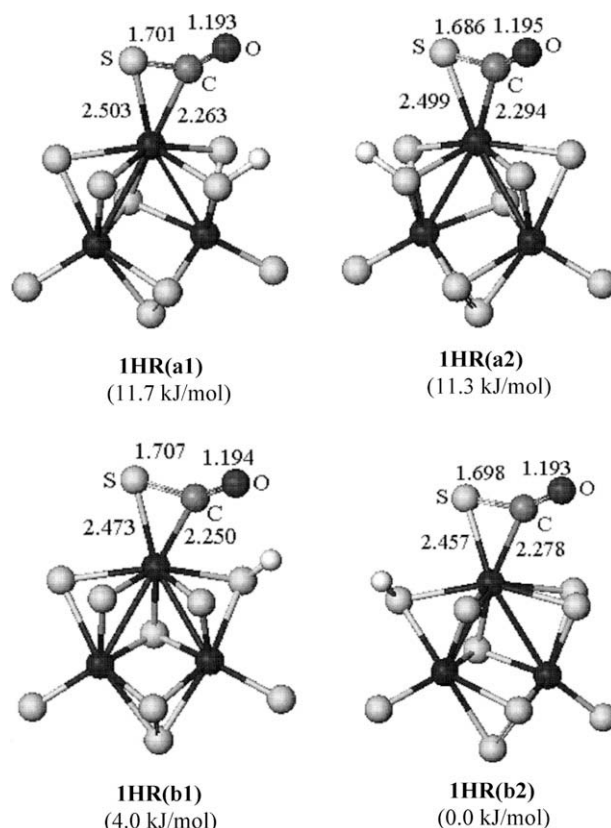

Fig. 3. Structures (Å) and relative energies (kJ/mol) of adsorbed COS on Mo_3S_9 cluster with hydrogen at different positions.

3.1.1. The hydrogenation of uncoordinated oxygen

Based on the adsorption structure **1HR(b1)** in Fig. 3, the calculation for the hydrogenation reaction of uncoordinated oxygen in COS was carried out. Following the LST/QST procedure, the transition state (**1HTS(1)**) connecting **1HR(b1)** and **1HP(1)** was

located and showed in Fig. 4 (top). The two S⋯H distances in **1HTS(1)** are 1.301 and 1.667 Å, respectively. The activation free energy of this step is 64.0 kJ/mol, and the reaction to the mono-hydrogenated product **1HP(1)** is endergonic by 54.2 kJ/mol.
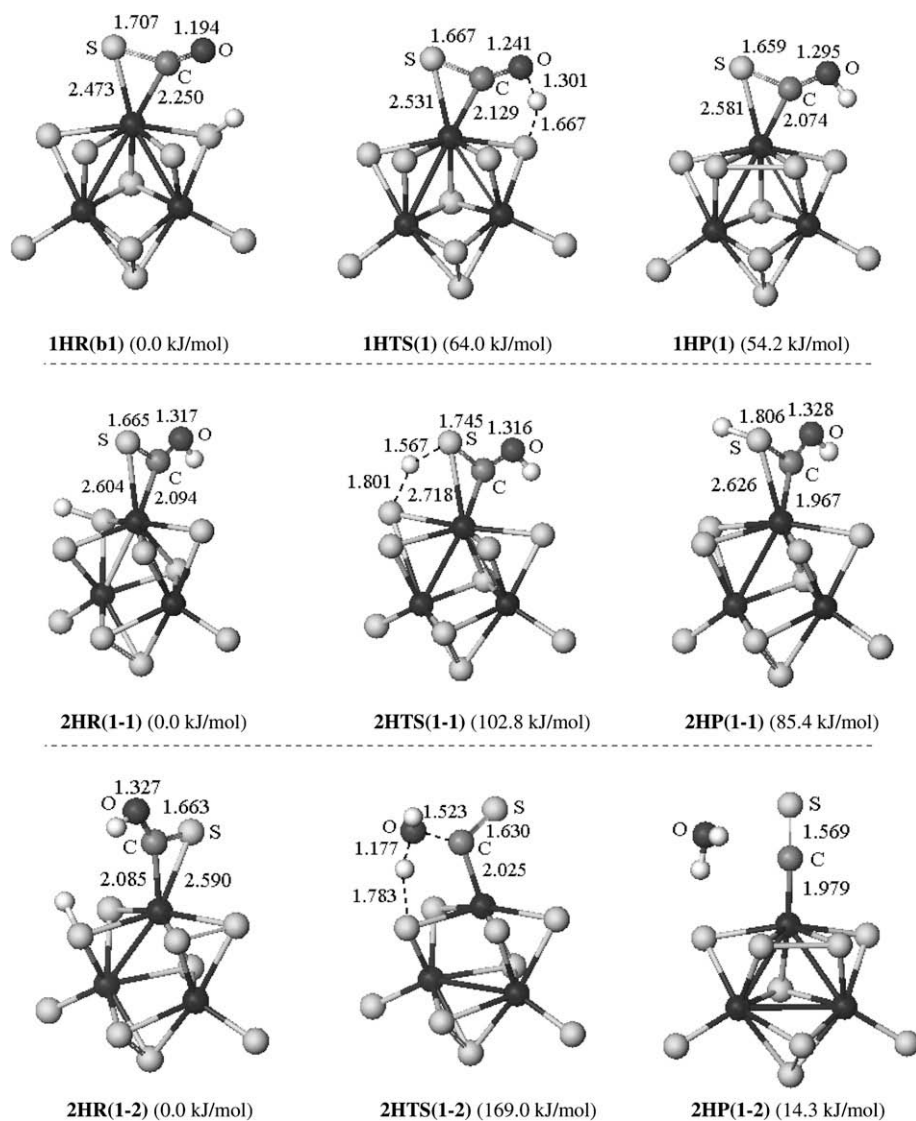

Fig. 4. Structures (Å) and free energies (kJ/mol) of the transition states and intermediates of the first (top) and the second (middle, bottom) H transfer processes for the hydrogenation of COS.
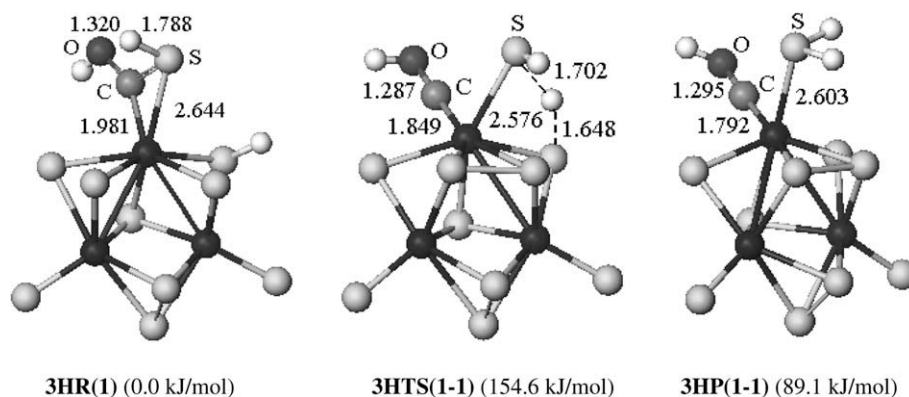

Fig. 5. Structures (Å) and free energies (kJ/mol) of the transition state and intermediate of the third H transfer processes for the hydrogenation of COS.

The further H addition to **1HP(1)** will form several different adsorption structures, and two possible structures **2HR(1-1)** and **2HR(1-2)** with H adsorbing on different S position are shown in Fig. 4 (middle) and (bottom). They will probably take place the further H transformation reaction. For **2HR(1-1)**, the subsequent H transfer forms the adsorption structure **2HP(1-1)** with two hydro-

gen atoms on O and S positions of COS, respectively. The two S...H distances in the transition state **2HTS(1-1)** are 1.567 and 1.801 Å. The activation and reaction free energy of this second step are 102.8 and 85.4 kJ/mol, respectively.

As shown in Fig. 4 (bottom), if one more hydrogen atom transfers to O of **1HP(1)**, it will lead to break of C–O bond and formation
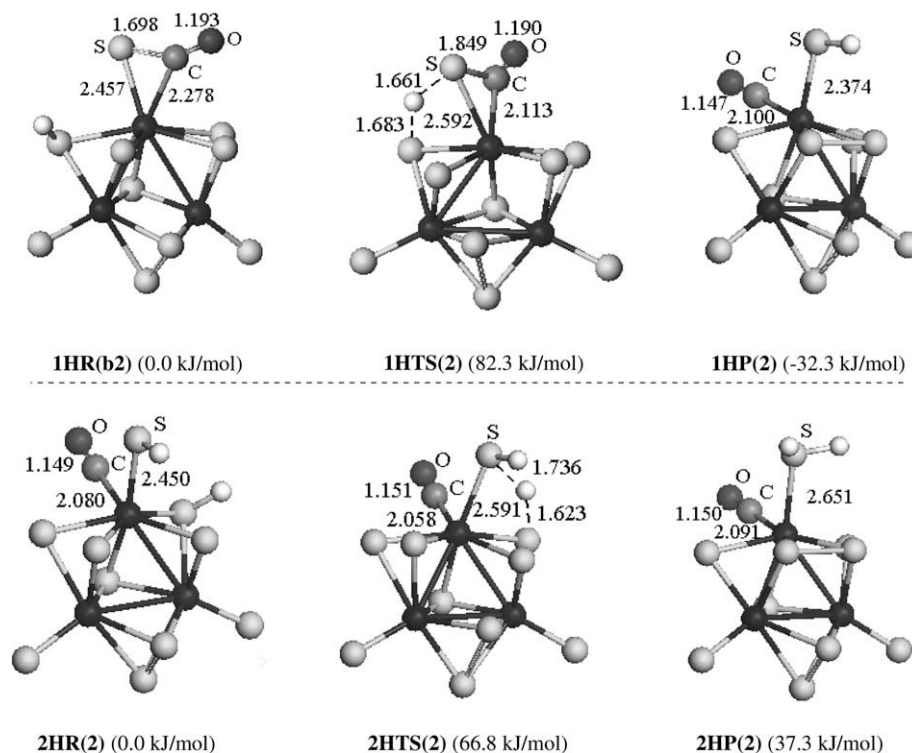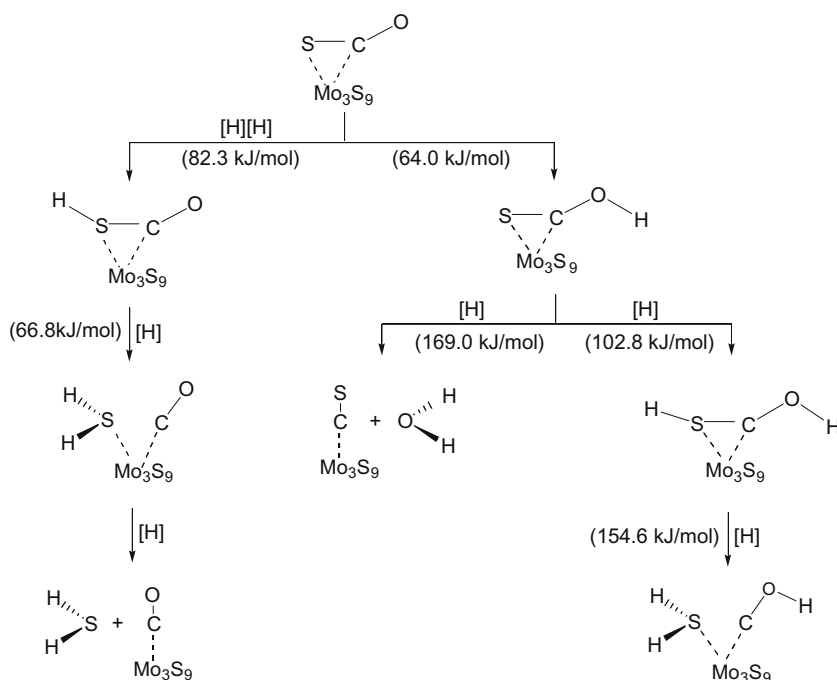

Fig. 6. Structures (Å) and free energies (kJ/mol) of the transition states and intermediates of the first (top) and the second (bottom) H transfer processes for the hydrogenation of COS.

Scheme 1. Investigated hydrodesulfurization reaction mechanisms for COS.

of H_2O through a transition state **2HTS(1-2)**. After this reaction, a CO adsorption structure on Mo_3S_9 is left. This step needs a higher free energy cost of 169.0 kJ/mol, and is endergonic (14.3 kJ/mol).

After a further H addition of **2HP(1-1)** to form **3HR(1)**, the subsequent H transfer in **3HR(1)** will lead to reaction as shown in Fig. 5. The transfer H attack SH group of **3HR(1)**, and forms an adsorbed H_2S and COH structure (Fig. 5). In transition state **3HTS(1-1)** of this step, the two S...H distances are 1.702 and 1.648 Å, respectively. The free energy barrier of the reaction is 154.6 kJ/mol. The H_2S in **3HP(1-1)** will desorb subsequently and leave an adsorbed COH structure which would form to adsorbed CO with probable H departure. There is no obviously transition state in desorption process of H_2S molecule found by energy scan calculations.

3.1.2. The hydrogenation of coordinated sulfur

The hydrogenation reactions for coordinated sulfur of adsorbed COS are shown in Fig. 6. Different with the first hydrogenation step of oxygen, reaction of sulfur in COS leads to formation of SH group along with C–S bond breaks directly. As illustrated in Fig. 6 (top), based on the structure. **1HR(b2)** with an adsorbed hydrogen on S(b) position near by the sulfur of COS, the H transformation to the S forms an adsorbed SH group and CO group through transition state **1HTS(2)**. The two S...H distances in **1HTS(2)** are 1.661 and 1.683 Å while the activation and reaction free energy of this step are 82.3 and −32.3 kJ/mol, respectively.

In Fig. 6 (bottom), a further H addition to **1HP(2)** will form reactant **2HR(2)** of next step. One more H transformation of **2HR(2)** with SH group leads to formation of an adsorbed H_2S on Mo_3S_9. In the transition state **2HTS(2)**, the two S...H distances are 1.736 and 1.623 Å, respectively. This step is with a 66.8 kJ/mol free energy cost. Both of adsorbed H_2S and CO will probably take place the desorption reaction. The H_2S will desorb as a final product. Based on energy scan result, the CO will have a similar energy increasing desorption process without transition state. However, the adsorbed CO will probably react with H to form different product such as alcohol or hydrocarbon with molybdenum sulfides as catalyst. The reactions are very complicated and beyond the scope of this paper, so will not be discussed here.

The possible pathways with different intermediates for above hydrodesulfurization reactions of COS were shown in Scheme 1. The computed free energies of activation and reaction for the individual steps are listed in Table 1. As shown in Scheme 1, in the path (i) of reaction, the hydrogenation of O is with lowest activation energy (64.0 kJ/mol) and will take place easily. In the following steps, no matter further hydrogenation of O and S, or departure of H_2S and H_2O will cost much higher energy (more than 100 kJ/mol). In the path (ii), the hydrogenation of S needs 82.3 kJ/mol energy cost.

Comparing with hydrogenation of O, it will be a little more difficult to take place, although the following departure of H_2S of this path will cost low activation energy (66.8 kJ/mol). Based on the computed free energy barriers of departure of H_2S (154.6 kJ/mol for path (i) and 66.8 kJ/mol for path (ii)) and H_2O (160.9 kJ/mol), it was found that the formation of H_2O is cost higher energy. This result indicated that the removal of S is easier to take place than that of O in reaction of COS. So, the favored catalytic pathway of COS is hydrogenation of O, then the departure of H_2S.

3.2. Reaction of CS_2 with Mo_3S_9 cluster

There are also four structures for adsorbed CS_2 on Mo_3S_9H as shown in Fig. 7: **1HR(a1)**, **1HR(a2)**, **1HR(b1)** and **1HR(b2)** with H adsorbing on the different position. They are close in energy with the largest difference of 10.2 kJ/mol. Only the reactions of **1HR(b1)** and **1HR(b2)** were consider for most steps.

The catalytic cycle of CS_2 is assumed to take place along two pathways: (i) hydrogenation of uncoordinated sulfur, (ii) hydrogenation of coordinated sulfur. The potential energy surface along hydrogenation of uncoordinated sulfur of CS_2 is computed firstly.

3.2.1. The hydrogenation of uncoordinated sulfur

The **1HR(b1)** in Fig. 7 is used as starting points for the reaction of uncoordinated sulfur of CS_2. Following the LST/QST procedure, the transition state **1HTS(1)** connecting **1HR(b1)** and **1HP(1)** was located and showed in Fig. 8 (top). The two S...H distances in **1HTS(1)** are 1.592 and 1.732 Å. The activation free energy of this step is 45.7 kJ/mol, and the reaction to the mono-hydrogenated product **1HP(1)** is endergonic by 12.4 kJ/mol.
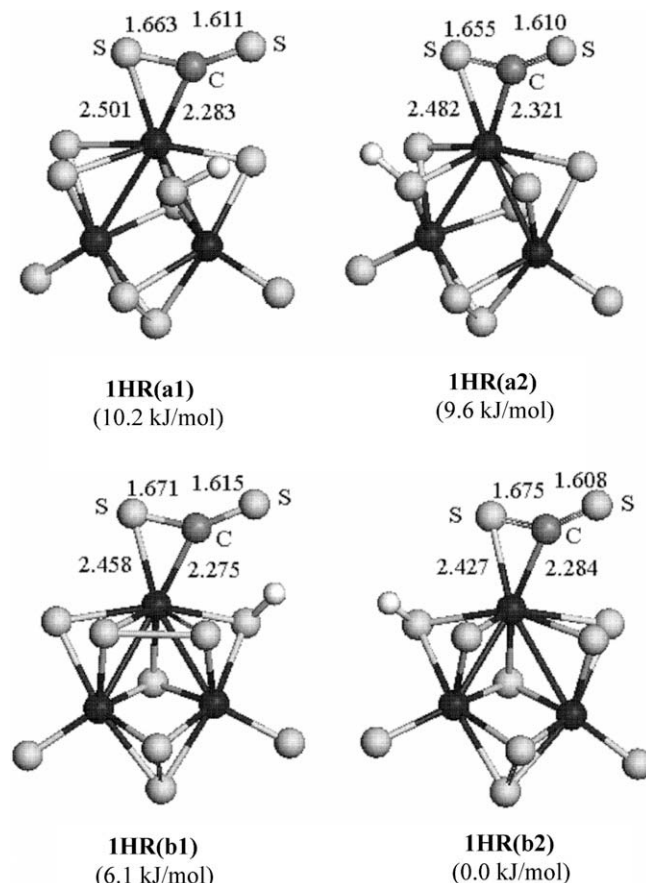

1HR(a1)
(10.2 kJ/mol)

1HR(a2)
(9.6 kJ/mol)

1HR(b1)
(6.1 kJ/mol)

1HR(b2)
(0.0 kJ/mol)

Fig. 7. Structures (Å) and relative energies (kJ/mol) of adsorbed CS_2 on Mo_3S_9H cluster with hydrogen at different positions.

Table 1
Gibbs free energies of activation ($\Delta G^{\ddagger}$, kJ/mol) and reaction (ΔG, kJ/mol) for COS and CS_2 at 550 K and 1 atm.

Elementary step	$\Delta G^{\ddagger}$	ΔG
COS		
1HR(b1) → 1HTS(1) → 1HP(1)	64.0	54.2
2HR(1-1) → 2HTS(1-1) → 2HP(1-1)	102.8	85.4
2HR(1-2) → 2HTS(1-2) → 2HP(1-2)	169.0	14.3
3HR(1) → 3HTS(1-1) → 3HP(1-1)	154.6	108.2
1HR(2) → 1HTS(2) → 1HP(2)	82.3	−32.3
2HR(2) → 2HTS(2) → 2HP(2)	66.8	37.3
CS₂		
1HR(b1) → 1HTS(1) → 1HP(1)	45.7	12.4
2HR(1-1) → 2HTS(1-1) → 2HP(1-1)	60.2	38.5
2HR(1-2) → 2HTS(1-2) → 2HP(1-2)	128.9	110.3
3HR(1) → 3HTS(1-1) → 3HP(1-1)	114.2	56.6
1HR(2) → 1HTS(2) → 1HP(2)	79.9	68.9
2HR(2) → 2HTS(2) → 2HP(2)	51.3	24.7

Like reaction of CS$_2$, further H addition of **1HP(1)** will form several different adsorption structures. By our test calculations, it was found that two possible structures **2HR(1-1)** and **2HR(1-2)** with H adsorbing on different positions shown in Fig. 8 (middle) and Fig. 8
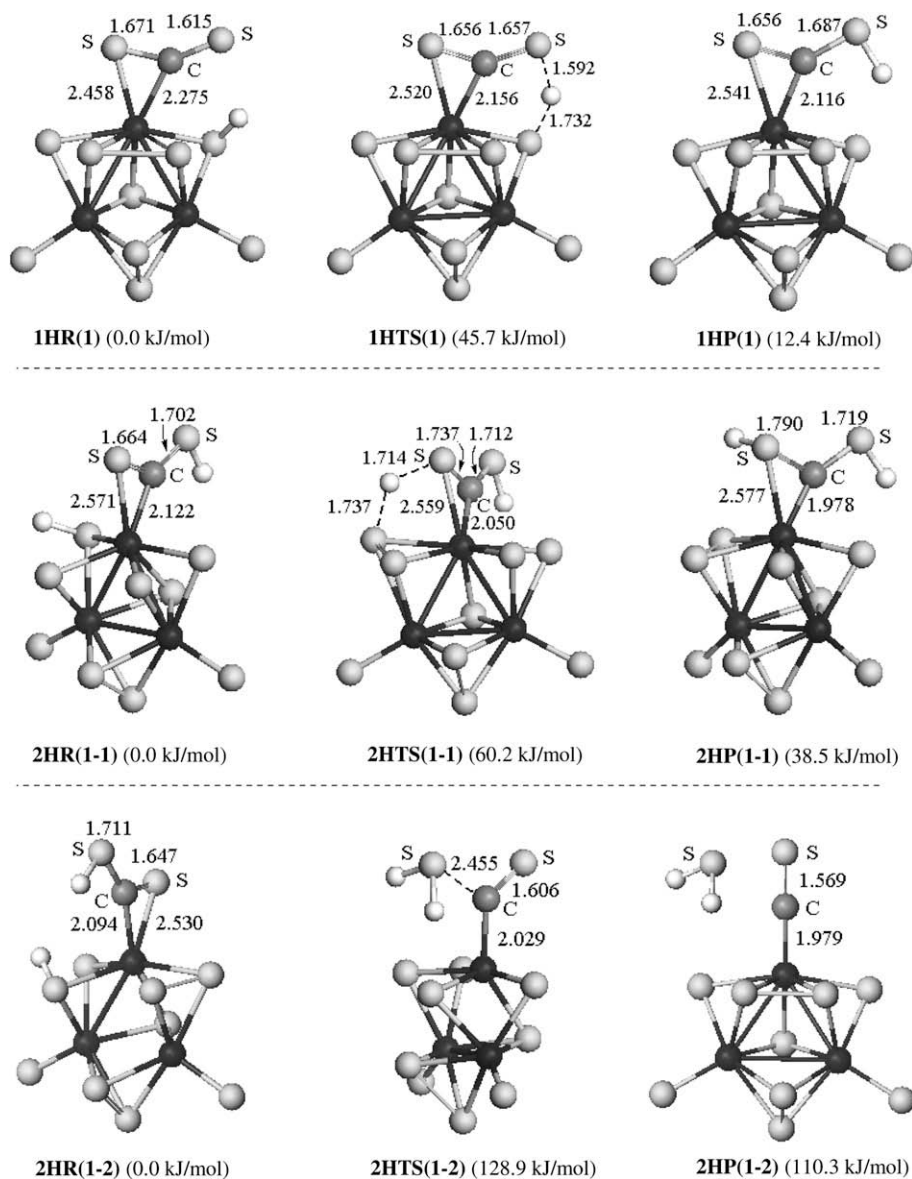

Fig. 8. Structures (Å) and free energies (kJ/mol) of the transition states and intermediates of the first (top) and the second (middle, bottom) H transfer processes for the hydrogenation of CS$_2$.
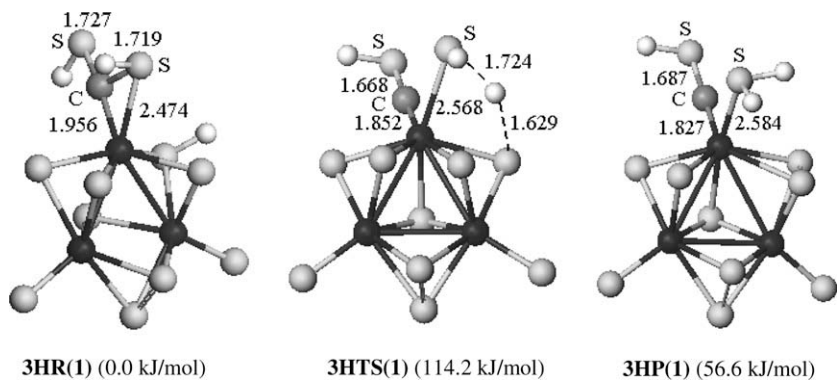

Fig. 9. Structures (Å) and free energies (kJ/mol) of the transition states and intermediates of the third H transfer processes for the hydrogenation of CS$_2$.

(bottom) will take place the further H transformation reaction. For **2HR(1-1)**, the subsequent H transfer forms the **2HP(1-1)** product with two hydrogen atoms on two different S positions of CS_2. The two S...H distances in the transition state **2HTS(1-1)** are

1.714 and 1.737 Å, respectively. This second step has an activation free energy of 60.2 kJ/mol, and is endergonic (38.5 kJ/mol).

As shown in Fig. 8 (bottom), transformation of two hydrogen atoms to same S of CS_2 will lead to break of one C–S bond and
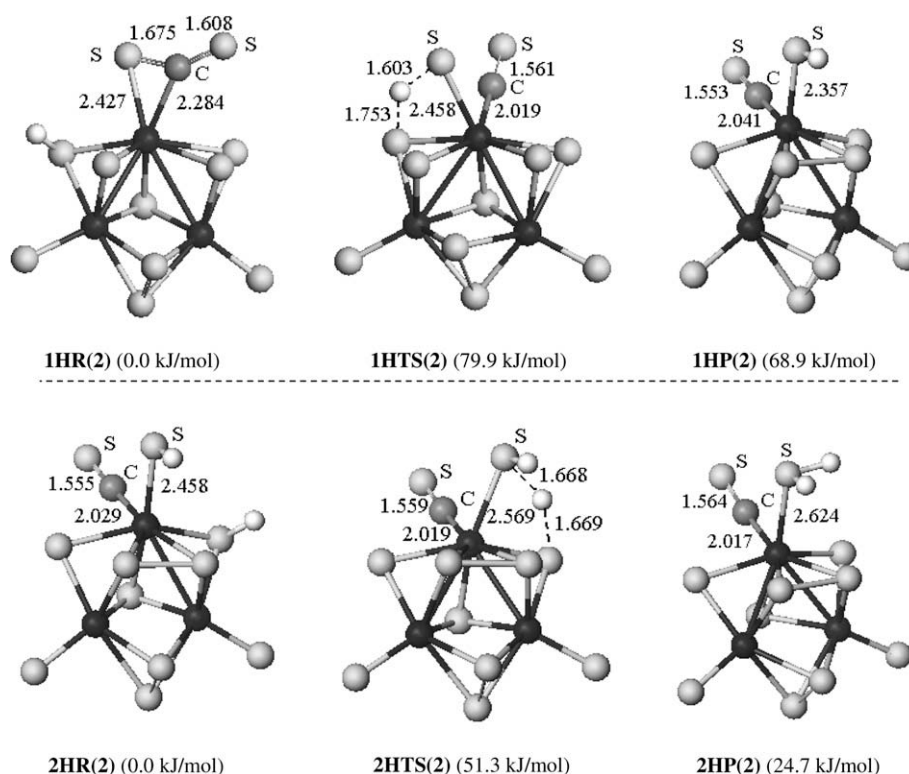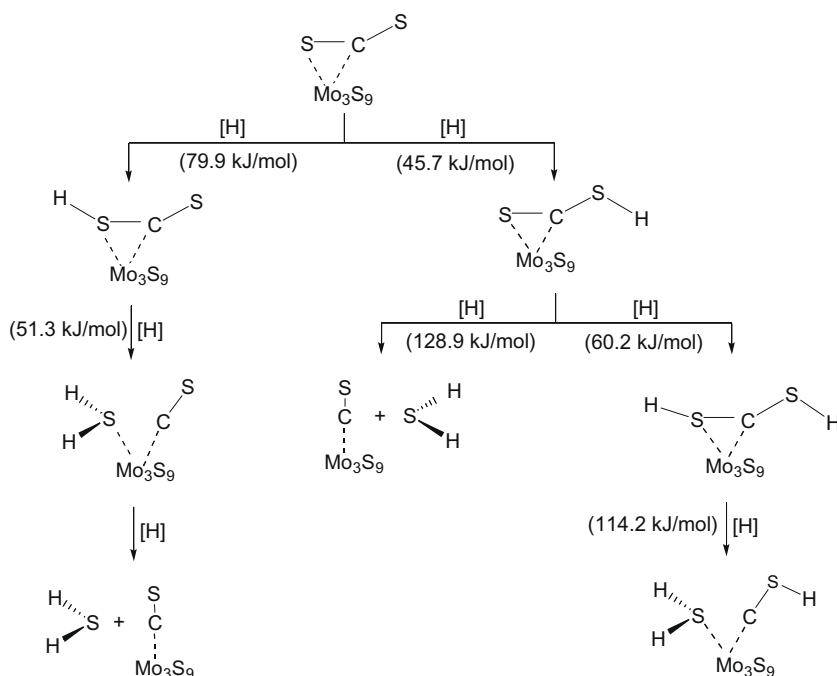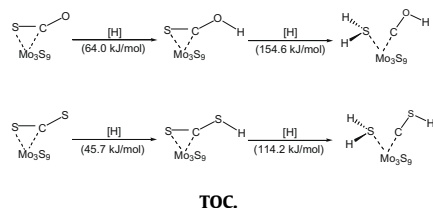

Fig. 10. Structures (Å) and free energies (kJ/mol) of the transition states and intermediates of the first (top) and the second (bottom) H transfer processes for the hydrogenation of CS_2.

Scheme 2. Investigated hydrodesulfurization reaction mechanisms for CS_2.

TOC.

the formation of H₂S through a transition state **2HTS(1-2)**, and a CS adsorption structure will be left. This reaction needs a higher free energy cost of 128.9 kJ/mol, and is also endergonic (110.3 kJ/mol).

The following step is further H addition to **2HP(1-1)** for the formation of **3HR(1)**, and the subsequent H transfer in **3HR(1)** will lead to reaction shown in Fig. 5. The transfer H reacts with one of SH group of **3HR(1)**, forms an adsorbed H₂S and CSH structure (Fig. 9). In the transition states **3HTS(1-1)**, the two S...H distances are 1.724 and 1.629 Å, respectively. After this step with 114.2 kJ/mol free energy barrier, the H₂S in **3HP(1-1)** will desorb and left an adsorbed CSH structure. There is no obviously transition state in desorption process of H₂S molecule. Energy scan shows that along with lengthening of distance between H₂S and Mo, the energy keep increasing.

3.2.2. The hydrogenation of coordinated sulfur

The hydrogenation reactions of coordinated sulfur of CS₂ are shown in the Fig. 10. Different with the uncoordinated sulfur, the first hydrogenation step of other sulfur of CS₂ leads to formation of SH group along with C–S bond breaks directly. As illustrated in Fig. 10 (top), based on the structure 1HR(b2) with an adsorbed hydrogen on S(b) position near by the coordinated sulfur, H transformation to the S forms adsorbed SH group and CS group through transition state **1HTS(2)**. In **1HTS(2)**, the two S...H distances are 1.603 and 1.753 Å. The activation and reaction free energy of this step are 79.9 and 68.9 kJ/mol, respectively.

Further H addition to **1HP(2)** will form **2HR(2)** structure shown in Fig. 10 (bottom). With a separated SH group, one more H transformation of **2HR(2)** will be much simpler and lead to formation of an adsorbed H₂S. In the transition state **2HTS(2)**, the two S...H distances are 1.668 and 1.669 Å, respectively. This step is with 51.3 kJ/mol free energy cost. Both of adsorbed H₂S and CS will probably take place the desorption reaction. The H₂S will be a final product, and desorb without obviously transition state as discussed above. Based on energy scan result, the CS will have a similar energy increasing desorption process without transition state. The desorption of CS on Mo₃S₉ cluster is with 135.3 kJ/mol free energy change.

The possible pathways for initial hydrodesulfurization reactions of CS₂ were shown in Scheme 2. The computed free energies of activation and reaction for the individual steps are listed in the Table 1. Similar with reaction of COS, the hydrogenation of uncoordinated S with lowest activation energy (45.7 kJ/mol) in the path (i) of CS₂ will take place more easily than that of coordinated S in path (ii) (79.9 kJ/mol activation energy). However, in the path (i), the further hydrogenations of S that will lead to departure of H₂S are with higher activation energies, such as 128.9, 114.2 kJ/mol, so will be a little difficult to take place. Based on the computed free energy barriers, it was found that the favored path of CS₂ is hydrogenation of uncoordinated S. Comparing with COS, CS₂ shows higher S removal reaction activity in this condition for lower activation energy costs (TOC).

In our previous study [29,30], the detailed HDS mechanisms of thiophenic compounds have been discussed, and this enables a comparison with that of COS and CS₂. The favored reaction path of thiophene is the direct formation of butadiene through intermediate 2,5-DHT. The computed activation free energy for thiophene

rate-determining step is 93.5 kJ/mol. For benzothiophene, the free energy barrier for the rate-determining step that is hydrogenolysis of intermediate DHBT is 121.4 kJ/mol. Comparing with thiophene and benzothiophene, COS and CS₂ shows lower reaction activity in same experimental condition. Based on our computed results, it could be found that while sulfur contents of thiophenic compounds in industrial feedstocks are hydrodesulfured by molybdenum sulfides catalyst, that of COS and CS₂ will also probably be removed.

4. Conclusions

In this work, hydrodesulfurization reaction mechanisms of COS and CS₂ with Mo₃S₉ cluster have been computed at the level of density functional theory. All species involved in the catalytic process and their relative free energies have been determined. The possible pathways with different intermediates for hydrodesulfurization reactions were analyzed, and the products include H₂S, H₂O, CO and CS. It was found that the hydrogenation reactions of uncoordinated S are with relatively low energy barrier and more favorable than other possible paths. In the computed conditions, molybdenum sulfides catalyst is effective for hydrodesulfurization of COS and CS₂, and CS₂ shows more reaction activity.

References

[1] (a) C. Willey, M. Iwao, R.N. Castle, M.L. Lee, Anal. Chem. 53 (1981) 400;
    (b) T. Kabe, A. Ishihara, H. Tajima, Ind. Eng. Chem. Res. 31 (1992) 1577.
[2] C. Rhodes, S.A. Riddel, J. West, B.P. Williams, G.J. Hutchings, Catal. Today 59 (2000) 443.
[3] B.C. Wiegand, C.M. Friend, Chem. Rev. 92 (1992) 491.
[4] F.P. Daly, J. Catal. 51 (1978) 221.
[5] E.J.M. Hensen, M.J. Vissenberg, V.H.J. de Beer, J.A.R. van Veen, R.A. van Santen, J. Catal. 163 (1996) 429.
[6] D.L. Sullivan, J.G. Ekerdt, J. Catal. 178 (1998) 226 and references therein.
[7] I.A. Van Parijs, G.F. Froment, Ind. Eng. Chem. Prod. Res. Dev. 25 (1986) 437.
[8] S. Cristol, J.-F. Paul, E. Payen, D. Bougeard, S. Clemendot, F. Hutschka, J. Phys. Chem. B 106 (2002) 5659.
[9] S. Cristol, J.-F. Paul, E. Payen, D. Bougeard, S. Clemendot, F. Hutschka, J. Phys. Chem. B 104 (2000) 11220.
[10] A. Travert, H. Nakamura, R.A. van Santen, S. Cristol, J.-F. Paul, E. Payen, J. Am. Chem. Soc. 124 (2002) 7084.
[11] P. Raybaud, J. Hafner, G. Kresse, S. Kasztelan, H. Toulhoat, J. Catal. 189 (2000) 129.
[12] P. Raybaud, J. Hafner, G. Kresse, S. Kasztelan, H. Toulhoat, J. Catal. 190 (2000) 128.
[13] H. Orita, K. Uchida, N. Itoh, J. Mol. Catal. A Chem. 193 (2003) 197.
[14] L.S. Byskov, M. Bollinger, J.K. Nørskov, B.S. Clausen, H. Topsøe, J. Mol. Catal. A Chem. 163 (2000) 117.
[15] X. Ma, H.H. Schobert, J. Mol. Catal. A Chem. 160 (2000) 409.
[16] A.H. Jubert, R. Pis Diez, G.L. Estiú, F. Ruette, J. Mol. Struct. (THEOCHEM) 465 (1999) 111.
[17] Y.-W. Li, X.-Y. Pang, B. Delmon, J. Mol. Catal. A Chem. 169 (2001) 259.
[18] I.I. Zakharov, A.N. Startsev, J. Phys. Chem. B 104 (2000) 9025.
[19] M. Neurock, R.A. van Santen, J. Am. Chem. Soc. 116 (1994) 4427.
[20] P. Raybaud, J. Hafner, G. Kresse, H. Toulhoat, Surf. Sci. 407 (1998) 237.
[21] P. Raybaud, J. Hafner, G. Kresse, H. Toulhoat, Hydrotreatment and Hydrocracking of Oil Fractions, Elsevier Science B.V., New York, 1999, p. 309.
[22] S. Helveg, J.V. Lauritsen, E. Lae Gsgaard, I. Stensgaard, J.K. Nørskov, B.S. Clausen, H. Topsøe, F. Besenbacher, Phys. Rev. Lett. 84 (2000) 951.
[23] S.P. Cramer, K.S. Liang, A.J. Jacobson, C.H. Chang, R.R. Chianelli, Inorg. Chem. 23 (1984) 1215.
[24] (a) A. Müller, E. Diemann, A. Branding, F.W. Baumann, M. Breysse, M. Vrinat, Appl. Catal. 62 (1990) L13;
    (b) J.L. Brito, F. Severino, N.N. Delgado, J. Laine, Appl. Catal. A 173 (1998) 193;
    (c) E. Diemann, T. Weber, A. Müller, J. Catal. 148 (1994) 288. and references cited therein.
[25] Th. Weber, J.C. Muijsers, J.W. Niemantsverdriet, J. Phys. Chem. 99 (1995) 9194.
[26] S.J. Hibble, M.R. Feaviour, M.J.J. Almond, Chem. Soc. Dalton Trans. (2001) 935.

[27] H. Jiao, Y.-W. Li, B. Delmon, J.-F. Halet, J. Am. Chem. Soc. 123 (2001) 7334.
[28] P.W. de Bont, M.J. Vissenberg, V.H.J. de Beer, J.A.R. van Veen, R.A. van Santen, A.M. van der Kraan, Appl. Catal. A 202 (2000) 99.
[29] X.-Q. Yao, H. Jiao, Y.-W. Li, J. Mol. Struct. (THEOCHEM) 726 (2005) 67.
[30] X.-Q. Yao, H. Jiao, Y.-W. Li, J. Mol. Struct. (THEOCHEM) 726 (2005) 81.
[31] Y. Dobrogorskaya, J. Mascetti, I. Papai, A. Nemukhin, Y. Hannachi, J. Phys. Chem. A 107 (2003) 2711–2715.
[32] J. Panek, Z. Latajka, J. Phys. Chem. A. 103 (1999) 6845.
[33] (a) B. Delmon, Catal. Lett. 22 (1993) 1;
(b) J.-F. Paul, E. Payen, J. Phys. Chem. B 107 (2003) 4057.
[34] (a) J.A. Rodriguez, S.Y. Li, J. Hrbek, H.H. Huang, G.Q. Xu, Surf. Sci. 370 (1997) 85;
(b) J.A. Rodriguez, J. Phys. Chem. B 101 (1997) 7524. and references cited therein.